

Interaction of the strong light field of a dye laser radiation with a two-level system

I. S. Zeřikovich, S. A. Pul'kin, and L. S. Gařda

Grodno State University

(Submitted 5 January 1984)

Zh. Eksp. Teor. Fiz. **87**, 125–134 (July 1984)

The paper reports an investigation of the changes that occur in the generation spectrum of a dye laser with atomic-barium vapor in the cavity resonator near the resonance absorption line ($\lambda = 553.5$ nm). It is shown that the changes in the generation spectrum are determined by the nature of the interaction between the strong light field of the radiation and the two-level system. The nonresonance and resonance interactions between the radiation and the two-level system are studied. It is shown that in the case of the nonresonance interaction the changes in the generation spectrum are due to the formation of a nonlinear frequency-dependent lens. In the case of the resonance interaction, it is found that the absorption line splits up into two components, and that the splitting increases linearly with increasing intensity of the light-wave field. There occurs between these components a spectral intensity amplification, which is interpreted as amplification, without population inversion, of the dye-laser radiation in the atomic-barium layer.

1. INTRODUCTION

Intensity amplification in the generation spectrum of a dye laser near the absorption line of atoms placed inside the cavity resonator has been studied in a large number of investigations.^{1–11} Two principal models have been theoretically and experimentally investigated for the spectral concentration of the radiation. One of these models assumes the existence in the absorbing medium of a frequency-dependent lens due to the nonuniform distribution of the excited atoms over the cross section of the medium, while the other model assumes the creation of a nonlinear frequency-dependent lens in the medium by the high-intensity light field. The investigations in which cw dye lasers with an intracavity absorption cell were used^{1,10} assume the natural lenticularity of the medium to be the principal mechanism responsible for the radiation concentration, while those in which high-power pulsed lasers were used^{5,11} assume the nonlinear lenticularity to be the principal mechanism. Back in 1973 Shank and Klein¹ formulated the chief characteristics of the "capture" of a frequency during work with cw dye lasers: the frequency capture occurs on both the short- and the long-wavelength sides of the absorption line; on the long-wavelength side the capture is frequency retuned when the gas pressure in the cell is changed; on the short-wavelength side the capture is immediately adjacent to the absorption line, and is not frequency retuned. Further theoretical investigations showed that the natural lenticularity of the medium can explain the capture only on the long-wavelength side of the absorption line. In Ref. 11 an account is given of an experimental and theoretical investigation of the effect of the radiation concentration on the susceptibility of the medium in the intracavity absorption cell. It is shown that the spectral concentration of the radiation on the short-wavelength side of the neon absorption line ($\lambda = 594.5$ nm) is due to self-action of the laser radiation in the neon. The theoretical analysis was carried out on the basis of the solution to the wave equation for a cavity partially filled with a medium describable by a generalized two-level model.

In the present paper we report investigations of the intensity amplification and weakening effects that occur in the

generation spectrum of a dye laser with atomic-barium vapor in the vicinity of the absorption line with wavelength $\lambda = 553.3$ nm. The corresponding resonance transition in the barium atom (the transition $6^1S_0 - 6^1P_1$) is a good approximation to a two-level system.

2. EXPERIMENTAL PROCEDURE

The investigations were carried out with the aid of the method of holographic interference spectroscopy developed by two of us (I. S. and S. A.),¹² and used in the investigation reported in Ref. 11. The method allows us to study the contour of the absorption line and the behavior of the refractive index near the absorption lines of the atoms in the intracavity absorption cell of a dye laser in the case of holographic processing of the intracavity spectrograms.

The transmission distribution of the initial spectrogram has the form

$$\tau \sim I_0 + I_0 \exp(-2k_\lambda l) + 2I_0 \exp(-k_\lambda l) \times \cos \left\{ \frac{2\pi x}{p_0} + \frac{4\pi [n(\lambda) - 1]}{\lambda} \right\}, \quad (1)$$

where k_λ is the absorption coefficient of the barium atoms, l is the thickness of the absorbing layer, p_0 is the period of the spectral bands of the empty cavity, x is the running coordinate in the dispersion direction of the spectrograph, and I_0 is the intensity in the empty arm of the cavity.

It follows from (1) that the spectral-band contrast

$$V(\lambda) = \frac{I_{\max} - I_{\min}}{I_{\max} + I_{\min}} = \frac{2 \exp(-k_\lambda l)}{1 + \exp(-k_\lambda l)}. \quad (2)$$

For $k_\lambda l \gg 1$,

$$V(\lambda) = \exp(-k_\lambda l), \quad (3)$$

i.e., the band contrast over the spectrum is determined by the absorption line contour. In the case when the spectrogram is illuminated by a coherent wave and the zeroth diffraction order is filtered out the intensity distribution in it is given by

$$I_{b0} \sim I_0 [1 + \exp(-2k_\lambda l)]. \quad (4)$$

Thus, the intensity distribution in the zeroth diffraction order characterizes the distribution of the initial intensity

over the spectrum, without the modulation introduced by the interference term.

The intensity distribution in the first diffraction order is given by

$$I_1 \sim V^2 = \exp(-2k_x l). \quad (5)$$

This intensity distribution reflects the spectral shape of the absorption line contour for the atomic medium.

3. EXPERIMENT

In the experiment, for the recording of the spectrograms, we used a dye laser with a Michelson cavity. The dye was pumped by the second harmonic of a rubidium laser (of power $\sim 200\text{--}400$ kW and pulse duration ~ 30 nsec) in the transverse scheme. The dye (coumarin 153) was in a quartz cuvette with windows cut at the Brewster angle, which ensured the linear polarization of the radiation. The vapor was obtained through the evaporation and dissociation of barium hydroxide in a variable-current arc discharge at two values of the current, 3–4 A and 10–12 A. The stand of a DG-2 arc generator was placed in one of the arms of the Michelson cavity. The thickness of the absorbing layer in the interelectrode gap ranged from 5 to 10 mm. The laser radiation was trained on a DFS-13 spectrograph. The entrance slit of the spectrograph was fully open, and the laser radiation was focused on the plane of the slit by a cylindrical lens. The intensity distribution in the exit plane of the spectrograph comprises, in the case of an empty cavity, equidistant spectral lines. The use of a cylindrical lens allowed us to obtain spectral lines at the rate of ~ 15 lines/mm, which is not possible in the case when the entrance slit is used.

The spectrograms were recorded on a "Mikrat-300" photographic film. The 15 lines/mm frequency allows us to easily filter out the first diffraction order from the zeroth, and eliminate the processing procedure errors connected with this order.

We studied at an arc current 3–4 A the variation of the intensity of the generation spectrum near the absorption line of barium atoms ($\lambda = 553.5$ nm) for different radiation intensities. The measured halfwidth of the absorption line is ~ 0.015 nm. The most typical results of the experiments are presented in Figs. 1a–1c. These figures (the upper parts) show photographs of the initial spectrograms. In Fig. 1a we can clearly see the following regions: on the short-wavelength side of the reference line ($\lambda = 553.5$ nm) we can see a bright region, which corresponds to the amplification of the radiation intensity, and on the long-wavelength side we can see a dark region, which corresponds to intensity diminution. In Fig. 1b (upper part) we can see three regions: a bright and a dark region on the short-wavelength side of the reference line ($\lambda = 553.5$ nm) and a dark region on the long-wavelength side of the reference line. The dark regions correspond to a weakening of the radiation, while the bright region corresponds to the intensification of the radiation. Figure 1c (the upper part) also clearly exhibits three regions of spectral variation of the radiation intensity, but the regions of spectral enhancement and diminution of the intensity located on the short-wavelength side of the absorption line are broader than the corresponding regions in Fig. 1b. Fig-

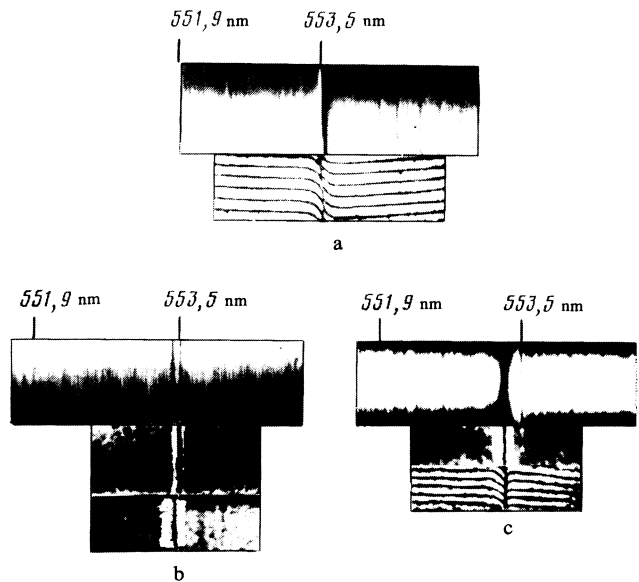


FIG. 1. Experimental results obtained in the holographic processing of the spectrograms: a) field broadening of the absorption line; b) and c) Stark shift of the absorption line for different intensities of the dye-laser radiation.

ures 1a and 1c (the lower parts) show photographs of the interference patterns obtained upon the illumination of the initial spectrograms by two coherent beams propagating at such angles to each other that they interfere after the filtration \pm the first light-diffraction orders on the spectrogram. The interference bands represent on some scale the dependence $n(\lambda) - 1$. It can clearly be seen in Fig. 1a that the center of the absorption line coincides with the reference line set on the initial spectrogram by the radiation emitted by the barium atoms in the arc.

A. Zones of variation of the generation spectrum in the case of field broadening of the absorption line

The shape of the interference bands shown in Fig. 1a (the lower half) corresponds to the behavior of $n(\Delta) - 1$ for a contour broadened by a light-wave field, and is given by the expression¹³:

$$n-1 = NfA \frac{\Delta}{1 + \Delta^2 + J/J_s}, \quad (6)$$

where N is the concentration of the excited atoms in the absorption cell, f is the oscillator strength of the transition under investigation, $A = 0.22 \times 10^{-16}$, $T = \gamma^{-1}$ is the reciprocal halfwidth of the absorption line, $\Delta = (\omega_0 - \omega)T$ is the detuning from the absorption line (ω is the running frequency and ω_0 is the frequency of the absorption line), $J = E^2$ is the radiation intensity, and $J_s = E_s^2$ is the saturating field intensity.

In the weak field limit (i.e., for $J = 0$) the expression (6) goes over into the usual Sellmeier formula. Thus, the peripheral low-intensity dye-laser radiation zone gives rise, on passing through barium vapor, to the usual Sellmeier behavior of the refractive index. The central, high-intensity radiation zone causes the refractive index to behave in the manner described by the expression (6). As a consequence, there is formed over the cross section of the radiation beam a fre-

quency-dependent refractive-index gradient that brings about frequency-dependent focusing or defocusing of the dye-laser radiation. Thus, the nonlinear characteristics of the susceptibility of the intracavity medium determine the frequency lenticularity of the atomic medium and the regions of spectral enhancement and diminution of the intensity of the dye-laser radiation.

Using (6), we easily obtain the refractive-index increment with respect to the normal dispersion given by the Sellmeier formula:

$$\delta(n-1) = NfA \left[\frac{\Delta}{1+\Delta^2+J/J_s} - \frac{\Delta}{1+\Delta^2} \right]. \quad (7)$$

In this case the condition for spectral enhancement of the intensity can be expressed as $\delta(n-1) > 0$ (condition for frequency-dependent focusing). For $\delta(n-1) < 0$ there should occur defocusing of the radiation, accompanied by spectral diminution of the radiation intensity. It follows from the expression (7) that focusing, with spectral enhancement of the intensity, occurs in the region $\Delta < 0$ (the short-wave region), while defocusing, with spectral diminution of the radiation intensity, occurs in the region $\Delta > 0$ (the long-wavelength region).

Figure 2 shows the plot (the continuous curve) of the dependence $n(\Delta) - 1$, obtained in the processing of the interference pattern shown in Fig. 1a (the lower part). In processing the interference pattern, we used the expression (6) and computed the values of $Nf \sim 10^{13}$ at/cm³ and $J/J_s \sim 10^3$. As is well known,¹⁴ for discharge in air, $J_s \sim 0.3$ esu ($S \sim 100$ W/cm²). From the Sellmeier formula we computed for the obtained Nf value the dependence $n(\Delta) - 1$, which is depicted in Fig. 2 by the dashed line. Subtracting one graph from the other, we easily obtain the regions of spectral enhancement and diminution of the intensity. The width of these regions are in good agreement with the width of the corresponding regions in the initial spectrogram in Fig. 1a (the upper part).

Figure 1b (the middle part) shows the pattern obtained upon the filtration of the zeroth light-diffraction order in the spectrogram. This pattern reproduces the radiation-intensity distribution in the vicinity of the absorption line. The intensity distribution is negative with respect to the photograph in Fig. 1b (the upper part), which is the positive of the initial intensity distribution. We can clearly see two bright

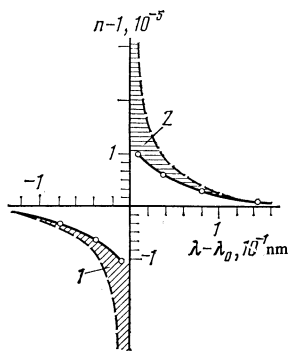


FIG. 2. Plots showing the positions of the regions of spectral amplification and weakening of the radiation under conditions of field broadening of the absorption line: 1) region of positive gradient and radiation amplification; 2) region of negative gradient and radiation weakening.

regions, which correspond to intensity reduction, separated by a dark region, which corresponds to intensity enhancement. Figure 1b (the lower part) shows the pattern obtained upon the filtration of the first light diffraction order in the spectrogram, which clearly exhibits the absorption line, displaced relative to the reference line by ~ 0.07 nm into the short-wavelength region.

Figure 1c (the middle part) also shows the pattern, which shows a ~ 0.19 -nm shift of the absorption line, obtained upon the filtration of the first light-diffraction order in the spectrogram. The mean radiation intensity is higher here than in the case (b) by roughly a factor of three. The interference pattern shown in Fig. 1c (the lower part) differs appreciably from the pattern shown in Fig. 1a (the lower part). The asymmetry in the behavior of $n(\Delta) - 1$ is clearly visible. Thus, there occur under the action of intense radiation a shift of the absorption line (the high-frequency Stark effect) and deformation of $n(\Delta) - 1$.

B. Zones of variation of the generation spectrum under conditions of a Stark shift of the absorption line

It is shown in Ref. 11 that, to explain a similar behavior of $n(\Delta) - 1$, we must use the generalized-two-level-model theory developed in Ref. 14, which takes account of the redistribution of the populations between the levels and the high-frequency Stark effect. The dependence $n(\Delta) - 1$ can, in the case of the single-photon resonance, be represented in the form

$$n(\Delta) - 1 = NfA \frac{JK(\vartheta - 1) + \Delta}{1 + (\Delta - JK)^2 + J/J_s}, \quad (8)$$

where JK is the high-frequency Stark shift, $K = h^{-1}(\chi^{22} - \chi^{11})T$ is the "repolarizability" parameter for the transition under investigation (the χ^{ij} denote the linear polarizabilities of the atom in the excited and ground states), and $\vartheta = 2\tau/T$, τ being the lifetime of the barium atom in the excited state. In our specific case $\tau \sim 10^{-8}$ sec, $T \sim 10^{-10}$ sec, and $\vartheta \sim 200$.

The expression (8) goes over into (6) in the case of a small Stark shift, i.e., for $JK \ll \Delta$. It should be noted that the formula (8) is valid for the stationary susceptibility, and is not, generally speaking, valid for the present experiment. But the qualitative character in the behavior of $n(\Delta) - 1$ is preserved. Using the expression (8), we easily obtain the refractive-index increment (for $\Delta \gg 1$):

$$\delta(n-1) = NfA \left[\frac{JK(\vartheta - 1)}{(\Delta - JK)^2 + J/J_s} - \frac{1}{\Delta} \right]. \quad (9)$$

From the expression (9) we can easily obtain the regions of spectral enhancement and diminution of the radiation intensity. The regions of spectral enhancement are given by the inequality

$$0 > \Delta > \frac{1 + J/J_s K^2}{J_s K(\vartheta + 1)}. \quad (10)$$

It follows from (10) that, for $K > 0$, there should be two focusing regions: one on the long-wavelength, and the other on the short-wavelength, side of the original absorption line. For $K < 0$ there is one focusing region, which abuts on the absorption line on the short-wavelength side.

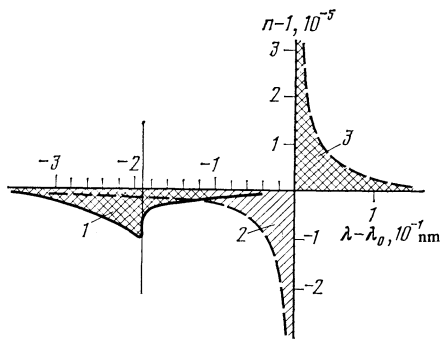


FIG. 3. Plots showing the positions of the regions of spectral variation of the radiation intensity under conditions of Stark shift of the absorption line: 1) and 3) regions of negative gradient and radiation weakening; 2) region of positive gradient and radiation amplification.

The regions of spectral diminution of the intensity are given by the inequality.

$$0 < \Delta < \frac{1 + JJ_s K^2}{J_s K (\vartheta + 1)}. \quad (11)$$

For $K > 0$ we have one defocusing region on the long-wavelength side of the absorption line, and for $K < 0$ we have two regions, one of which is located on the short-wavelength side of the absorption line ($\Delta < -(1 + JJ_s K^2)/J_s |K| (\vartheta + 1)$), while the other is located on the long-wavelength side ($\Delta > 0$).

In the experiment with barium vapor, $K < 0$ (the absorption line shifts into the short-wavelength region), and, consequently, there should, according to (10) and (11), be two regions of intensity attenuation and one region of enhancement, which is what is observed in experiment. For quantitative estimates let us use the following data. For Fig. 1b, $JK \sim 0.4 \times 10^2$; for Fig. 1c, $JK \sim 1.2 \times 10^2$, $K \sim 10^{-3}$. Then for Figs. 1b and 1c the beginnings of the defocusing regions will be defined as $\Delta < -20$ ($\Delta \lambda < -0.03$ nm) and $\Delta > 0$. Since $JJ_s K^2 \ll 1$, the beginnings of the defocusing regions depend weakly on the radiation intensity, but the width of the regions depends essentially on the intensity.

Figure 3 shows plots of the dependence $n(\Delta) - 1$: the continuous line is the plot obtained in the processing of the interference pattern shown in Fig. 1c (the lower part), while the dashed line is the theoretical graph computed from the Sellmeier formula ($N_f \sim 10^{13}$ at/cm³). The regions of spectral variation of the intensity are obtained by subtracting one graph from the other. The widths and positions of these regions are in good agreement with the widths and positions of the corresponding regions in the original spectrogram in Fig. 1c (the upper part).

It should be noted that the character of the spectral concentration is qualitatively preserved in the case of a high frequency of the spectral bands (~ 15 lines/mm) when the empty arm of the Michelson cavity is shut off. This indicates, that at such a frequency, the Stark shift of the absorption line is not caused by the modes of the Michelson cavity, but is determined by the spectral "unevenness" of the dye-laser radiation intensity, which undergoes more-than-an-order-of-magnitude fluctuations in different parts of the generation spectrum. It is well known¹⁵ that the nonmonochroma-

tic line near the absorption contour causes a Stark shift practically equivalent to the effect of the monochromatic component.

To estimate the focal length f_l of the nonlinear lens that arises in the absorbing layer of barium atoms under the action of the high-power radiation, let us use the results obtained in Ref. 16. If the refractive-index distribution in the medium is given by the expression

$$n(x, y) = n_0 [1 - \frac{1}{2} \alpha^2 (x^2 + y^2)], \quad (12)$$

where n_0 is the value of the refractive index on the optical axis and α is some complex parameter, then

$$f_l = \pi / 2\alpha, \quad (13)$$

and the radius w_f of the constriction region of the Gaussian beam is equal to

$$w_f = (\lambda / \pi \alpha n_0)^{1/2}. \quad (14)$$

The parameter α can be estimated from the refractive-index gradient δn between the center and the edge of the beam:

$$\alpha = (2\delta n / n_0 r_0^2)^{1/2},$$

where r_0 is the radius of the initial beam ($r_0 \sim 0.015$ cm) and $\delta n \sim 10^{-6}$. Then from (13) and (14) we find that $f_l \sim 20$ cm and $2w_f \sim 0.02$ cm.

C. Resonant interaction of the radiation with a two-level system

Another series of experiments were performed in which the barium vapor was obtained through the evaporation and dissociation of barium hydroxide in a 10–12 A arc discharge. The halfwidth of the absorption line is ~ 0.06 nm. The frequency of the bands of the generation spectrum was reduced to 4–5 lines/mm. In this case the halfwidth of the Michelson-cavity mode is ~ 0.02 nm. Figure 4a shows a photograph of

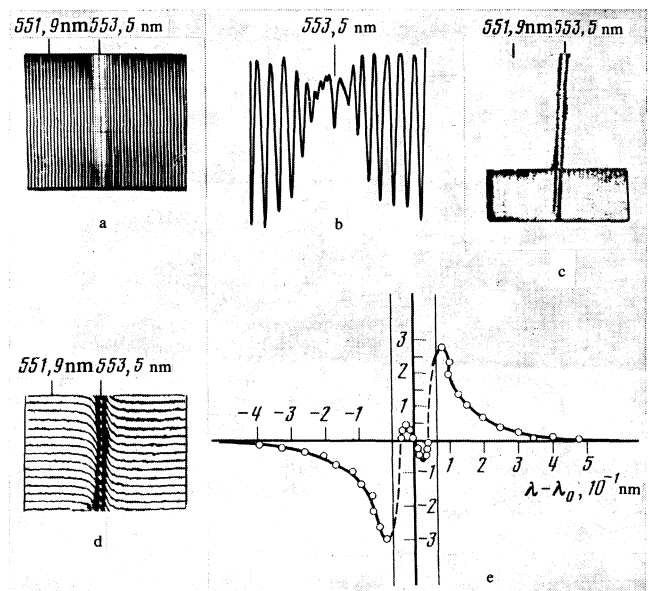


FIG. 4. Experimental results obtained in the case of resonance interaction of the radiation with a two-level system: a) the initial spectrogram; b) the densitogram of this spectrogram; c) splitting of the absorption line; d) interference-dispersion pattern; e) plot of the dispersion-induced variation of $[n(\lambda) - 1]$ in the vicinity of the split absorption line.

the initial spectrogram. The intensity of the spectrum is found to increase symmetrically with respect to the position of the unshifted absorption line corresponding to the resonance transition ($\lambda = 553.5$ nm). Figure 4b shows the densitogram of this spectrogram. Figure 4c (the upper part) shows the pattern obtained upon the filtration of the first light-diffraction order in the spectrogram. We can clearly see a symmetric—with respect to the reference line—splitting of the absorption line into two components (a ± 0.1 -nm splitting). Figure 4c (the lower part) shows the pattern obtained upon the filtration of the zeroth light-diffraction order in the spectrogram, and characterizing the intensity distribution in the generation spectrum. We can clearly see the intensity-enhancement regions, located symmetrically with respect to the reference line between the absorption lines. In Fig. 4d we show the interference pattern resulting from the interference of the \pm first light-diffraction orders in the spectrogram. Figure 4e shows the plot of the dependence $n(\lambda) - 1$ obtained in the processing of the interference pattern shown in Fig. 4d. The two vertical lines located symmetrically with respect to the original absorption line ($\lambda_0 = 553.5$ nm) indicate the centers of the splitting components.

The results obtained can be explained on the basis of the model of a two-level system located in a resonance-radiation field.¹⁷ This model predicts: 1) a symmetric splitting of the absorption line into two components; 2) a symmetric (with respect to the reference line) increase in the intensity as a result of negative absorption by the barium atoms (amplification without population inversion). Let us note that amplification without population inversion has been observed before in the radio-frequency region.^{18,19} The behavior of the refractive index (Figs. 4d and 4e) also corresponds qualitatively to the resonant-splitting model. To verify this surmise, we obtained and processed several spectrograms for different radiation intensities. In Fig. 5 we present the experimental data, obtained with the aid of a microphotometer, showing the dependence of the normalized (to the minimum value) magnitude of the splitting on the normalized (to the minimum value) magnitude of the field intensity at the intensity peaks of the Michelson-cavity modes. We show on the graph the intensity spread in the generation modes (the lengths of the horizontal lines). The experimental data are well approximated by a linear dependence, which demonstrates the resonant character of the splitting. The maximum

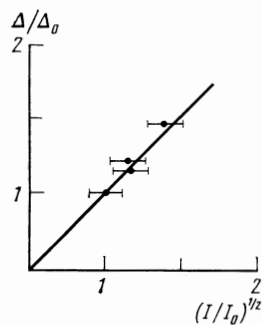


FIG. 5. Dependence of the normalized splitting Δ/Δ_0 of the absorption line (the distance between the splitting components) on the normalized amplitude $(I/I_0)^{1/2}$ of the dye-laser radiation field.

splitting is $\sim \pm 0.1$ nm; the minimum splitting, $\sim \pm 0.05$ nm. Let us estimate the Rabi frequency from the formula $\Omega = \pm d_{12}E/\hbar$, where d_{12} is the dipole moment of the transition. For the chosen transition $d_{12} \sim 10^{-17}$ esu. Then $E \sim 3 \times 10^4$ V/cm, which corresponds to an intensity of $I \sim 2 \times 10^6$ W/cm².

In the experiment we measured at the output end of the dye laser the radiation power, which was found to be ~ 100 kW. Furthermore, we photographed at the output end of the cavity the lasing spot, from which we estimated the lasing-spot diameter, which was found to be ~ 0.03 cm. To the measured values of the power and area of the lasing spot corresponds an intensity of $\sim 10^8$ W/cm². The intensity I_λ per spectral mode is $\sim 10^6$ W/cm², which agrees with the estimate for the Rabi frequency.

Still unclear is the question of the monochromaticity requirement for the exciting radiation in the case of resonance interaction.

4. CONCLUSION

It has been shown that the spectral amplification and weakening of the radiation of a high-power dye laser with barium vapor in the cavity are determined by the interaction between the strong light field of the radiation and the two level system. Three main situations have been considered:

1) the light-wave field causes broadening of the absorption contour and a symmetric "constriction" of the dispersion curve, which leads to the appearance of a converging lens in the region on the short-wavelength, and a diverging lens in the region on the long-wavelength, side of the absorption line; the position of these regions does not depend on the concentration of the atoms;

2) the "unevenness" of the intensity in the generation spectrum of the dye laser causes a Stark shift of the absorption line and an asymmetric deformation of the dispersion curve. In this case the spectral regions where the converging and diverging lenses arise are determined largely by the difference between the polarizabilities of the levels involved in the transition in question and the radiation intensity. They are given by the expressions (10) and (11); the position of these regions does not depend on the concentration of the atoms, but the focal power of the nonlinear lenses depends essentially on the concentration of the excited atoms;

3) when the halfwidth of the absorption line is ~ 0.06 nm we observe: a splitting of the absorption line into two components symmetrically located with respect to the original absorption line; the magnitude of the splitting linearly increases with increasing intensity of the light-wave field, which attests the resonance character of the splitting; the magnitude of the splitting does not depend on the concentration of the atoms; there occurs in the region between the split components a spectral intensity enhancement, which is symmetric with respect to the original absorption line, and which is interpreted as amplification (without population inversion) of the dye-laser radiation in the atomic-barium layer.

The possibility of constructing amplifiers and lasers operating on a two-level system without population inversion

under conditions of applied high-power radiation field is discussed in Ref. 19.

In conclusion we express our gratitude to A. M. Lyalikov for his help in the performance of the experiments.

- ¹C. V. Shank and M. B. Klein, *Phys. Lett.* **23**, 156 (1973).
²Y. H. Meyer, *Opt. Commun.* **19**, 343 (1976).
³Y. H. Meyer, *Opt. Commun.* **30**, 75 (1980).
⁴A. I. Rubinov, M. V. Belokon', and A. V. Adamushko, *Kvantovaya Elektron. (Moscow)* **6**, 723 (1979) [*Sov. J. Quantum Electron.* **9**, 433 (1979)].
⁵Y. Khanin, A. Kagan, V. Novikov, I. Polushkin, and A. Shcherbakov, *Opt. Commun.* **32**, 456 (1980).
⁶J. P. Reilly and G. C. Pimentel, *Appl. Optics* **15**, 2372 (1976).
⁷Y. H. Meyer, C. Loth, and R. Astier, *Opt. Commun.* **19**, 101 (1976).
⁸P. A. Apanasevich, A. A. Afanas'ev, and A. I. Urbanovich, *Kvantovaya Elektron. (Moscow)* **9**, 827 (1982) [*Sov. J. Quantum Electron.* **12**, 522 (1982)].
⁹A. J. de Tourton-Bruyns, H. A. Van der Leit, and A. Donozelman, *Physica (Utrecht) C* **95**, 825 (1978).
¹⁰M. V. Danileiko, A. M. Negriiko, and A. P. Yatsenko, *Kvantovaya Elektron. (Moscow)* **10**, 1660 (1983) [*Sov. J. Quantum Electron.* **13**, 1091 (1983)].
¹¹S. S. Anufrik, I. S. Zeĭlikovich, V. G. Kukushkin, and S. A. Pul'kin, *Kvantovaya Elektron.* **10**, 2053 (1983) [*Sov. J. Quantum Electron.* **13**, 1367 (1983)].
¹²I. S. Zeĭlikovich and S. A. Pul'kin, *Opt. Spektrosk.* **53**, 588 (1982) [*Opt. Spectrosc. (USSR)* **53**, 349 (1982)].
¹³A. Gavan and P. Kelley, *IEEE J. Quantum Electron.* **QE-2**, 470 (1966).
¹⁴V. S. Butylkin, A. E. Kaplan, Yu. G. Khronopulo, and E. I. Yakubovich, *Rezonansnoe vzaimodeĭstvie sveta s veshchestvom (Resonance Interaction of Light with Matter)*, Nauka, Moscow, 1977, Chap. II.
¹⁵A. M. Bonch-Bruevich, S. G. Przhibel'skiĭ, V. A. Khodovoĭ, and N. A. Chigir', *Zh. Eksp. Teor. Fiz.* **70**, 445 (1976) [*Sov. Phys. JETP* **43**, 230 (1976)].
¹⁶A. Gerrald and J. M. Burch, *Introduction to Matrix Methods in Optics*, Wiley-Interscience, New York, 1975 (Russ. Tansl., Mir, Moscow, 1978, p. 165).
¹⁷S. G. Rautian, and I. I. Sobel'man, *Zh. Eksp. Teor. Fiz.* **41**, 456 (1961) [*Sov. Phys. JETP* **14**, 328 (1962)].
¹⁸D. N. Klyshko, Yu. S. Konstantinov, and V. S. Tumanov, *Izv. Vyssh. Uchebn. Zaved. Radiofiz.* **8**, 513 (1965).
¹⁹A. M. Bonch-Bruevich, V. A. Khodovoĭ, and N. A. Chigir', *Zh. Eksp. Teor. Fiz.* **67**, 2069 (1974) [*Sov. Phys. JETP* **40**, 1027 (1975)].

Translated by A. K. Agyei